VOLCANIC FLOODING EXPERIMENTS IN IMPACT BASINS AND HEAVILY CRATERED TERRAIN USING LOLA DATA: PATTERNS OF RESURFACING AND CRATER LOSS. Jennifer L. Whitten[1], James W. Head[1], Gregory A. Neumann[2], Maria T. Zuber[3] and David E. Smith[3]. [1]Department of Geological Sciences, Brown University, Providence RI 02912 USA; (jennifer_whitten@brown.edu), [2]NASA Goddard Space Flight Center, Greenbelt, MD 20771, USA, [3]Department of Earth, Atmospheric and Planetary Sciences, Massachusetts Institute of Technology, Cambridge, MA 02139 USA.

Introduction: Terrestrial planetary bodies are characterized by extensive, largely volcanic deposits covering their surfaces. On Earth large igneous provinces (LIPs) abound, maria cover the nearside of the Moon, and volcanic plains cover large portions of Venus, Mars and Mercury [e.g., 1-5]. These large volcanic deposits can cover vast areas, between 10^3 and 10^6 km^2 [6]. The addition of such large quantities of material can significantly alter the surface by adding loads, obscuring primary crusts, and altering the atmosphere. Vital to understanding these effects is the ability to measure the volume of volcanic material emplaced, its age, and its flux. Although area is relatively easily measured, volumes are less certain due to often-poor understanding of thickness and the topography of the flooded substrate. New altimetry data provide key insights into the nature of this often-buried substrate and using this we can perform flooding experiments to estimate volumes more accurately and help decipher planetary thermal and geologic history.

The Moon provides an excellent setting for studying large volcanic deposits due to the large number of new, high-resolution image and altimetry datasets available. The work reported here builds on previous lunar flooding experiments [7]; we use the latest datasets to artificially flood three different locations of approximately the same size (~3.2 x 10^5 km^2), 1) the most heavily cratered lunar terrain [8], 2) Hertzsprung basin and 3) the Central Highlands (Figure 1), to understand both the thickness and volume of volcanic material required to form mare-like smooth deposits. Comparing these three regions permits a better understanding of the effect of volcanic flooding on pre-existing cratered terrains. Analysis of patterns of burial and preservation of craters created by this artificial volcanic flooding, as well as the change in crater size-frequency distributions, aids in identifying regions flooded by volcanic material on other terrestrial planets.

Data and Methods: Lunar Orbiter Laser Altimeter (LOLA) data [9, 10] are used to artificially flood the three regions selected for study. Both LOLA and Lunar Reconnaissance Orbiter Camera (LROC) data [11] are used for crater counts. Initially LOLA data are used to count craters at each flooding interval; these counts are then verified with LROC image data. Topography data at ~237 m/pixel is used as a basemap to flood the regions in 0.5 km increments. Two different methods of flooding are used: 1) Point source flooding is modeled using the Flood Landscape Analyst program, an ArcMap extension (Dongquan Zhao; Tsinghua University, Beijing); 2) Ubiquitous source vents; here flooding occurs simultaneously throughout a particular region and begins at the lowest elevation. At each flooding interval several data points are recorded including the volume of flooded material, the area covered (Figure 2) and the remaining exposed craters (Figure 3). Craters are only considered buried when their entire rim is covered with volcanic flood material. Cumulative frequency plots of the crater size-frequency distributions (CSFDs) are made to document the evolution of the CSFD with continued flooding.

Results: The pattern of flooding and observed changes in area and CSFD are most similar between the heavily cratered terrain and the Central Highlands, owing to their similar geometries. In both models the change in volume is similar in all three regions.

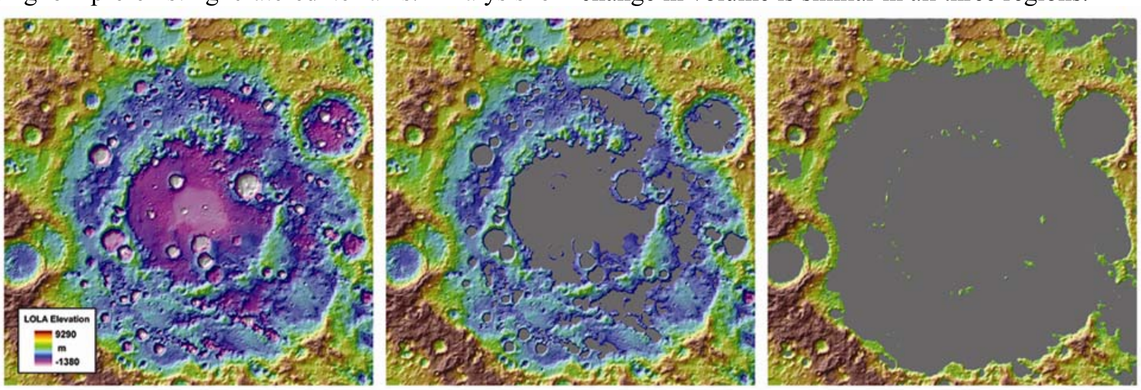

Figure 1. Results of the Hertzsprung ubiquitous flooding model. Left: Image shows the basin before the flooding experiments. Center: Image is flooded to 2 km elevation. Right: Image is the basin flooded to 4 km. Flooding intervals shown here correspond to those in Figure 3. LROC WAC (100 m/pixel) mosaic is overlain by 237 m/pixel LOLA data.

Heavily Cratered Terrain and Central Highlands: The CSFDs show significant changes in the smallest crater populations initially. With continued flooding larger and larger craters begin to disappear until only the largest are left before complete flooding of the region. The difference in the CSFDs between the point and ubiquitous flooding methods is the speed at which the smallest craters are removed. In the ubiquitous flooding method small craters are removed gradually while in the point source method a large portion of small craters are removed only after the larger craters (≥30 km diameter) have been completely flooded.

Hertzsprung Basin: This region has a relief range of approximately 11 km, with 6 km of flooding necessary to completely bury the innermost ring of the basin [12]. The first craters to completely disappear are those between 30 and 60 km diameter. This is due to the geometry of the region; craters located within the basin are covered before those just outside the basin rim. Therefore, the population of craters within the basin rim, large and small, disappears first.

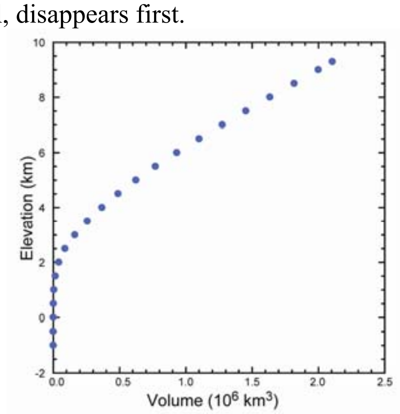

Figure 2. Elevation verses volume graph for the ubiquitous model applied to the Hertzsprung Basin region.

Conclusions: These flooding experiments indicate that there are three primary stages in large-scale volcanic flooding events. Phase 1: Many of the larger, fresher craters (≥30 km diameter) in a region begin to flood; flooding proceeds more vertically than laterally during this period. Phase 2: Once these deep craters are filled, volcanic material begins to flood relatively flat areas adjacent and between them, and lateral spreading exceeds vertical accumulation. Phase 3: Continued eruption of volcanic material leads to thickening of the deposits and burial of the largest craters as lateral spreading wanes and vertical accumulation dominates (Fig. 2).

A comparison of the two different flooding methods shows little difference in the volume of material emplaced or the evolution of the CSFD (Fig. 3). Most of the observed variation occurs in the preliminary stages of flooding. Initially, small craters are continually buried in the ubiquitous-source model while their population does not show much change in the point-source model until the larger crater rims are breached.

Perspective on the volumes of these deposits is enhanced by comparison to natural eruptions: Single eruptions are unlikely to produce the total volumes observed in these flooding experiments. Measurements of terrestrial flow volumes are used to estimate the number of eruptive events necessary to produce deposits of these measured volumes. Using a typical value of 2000 km^3 [6] yields between 7,500 to 10,500 individual events for the three flooded regions. Volume estimates for lunar flows [13] indicate between 185 and 70,000 individual events. We are currently applying these techniques to the Orientale and South Pole-Aitken (SPA) basin interiors in order to assess the early history of volcanism in SPA. CSFD data are being used to compare the differences between the Moon and Mercury to assess the role of volcanic resurfacing during the period of impact basin formation [e.g., 14]. Volume data will be important in assessing volcanic loads on the early lunar lithosphere that can be used in interpreting Gravity Recovery and Interior Laboratory (GRAIL) mission data.

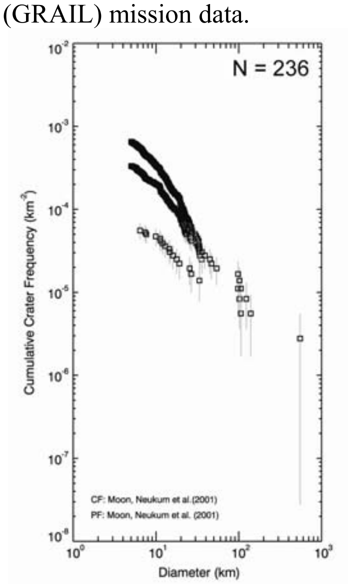

Figure 3. Three stacked CSFDs taken from the Hertzsprung Basin ubiquitous flooding model. Top CSFDs includes all craters counted, middle CSFD includes all exposed craters at 2 km and last CSFD shows all craters exposed at 4 km.

References: [1] Coffin M. F. and Eldholm O. (1994) *Rev. Geophys. 32,* 1-36. [2] Hiesinger H. et al. (2011) *GSA Spec. Pap. 477,* 1-51. [3] Phillips R. J. et al. (1992) *JGR* 97, 15923–15948. [4] Head J. W. et al. (2006) *Geology 34,* 285-288. [5] Head J. W. et al. (2011) *Science 333,* 1853–1856. [6] Parfitt E. A. and Wilson L. (2008) *Fundamentals of Phys. Volcanology*, 230 pp. [7] Head J. W. (1982) *Moon and Planets 26,* 61-88. [8] Head J. W. et al. (2010) *Science 17,* 1504-1507. [9] Zuber M. T. et al. (2010) *Space Sci. Rev. 150,* 63-80. [10] Smith D. E. et al. (2010) *Space Sci. Rev. 150,* 209-241. [11] Robinson M.S. et al. (2010) *Sci. Rev. 150,* 81-124. [12] Baker D.M.H. et al. (2011) *Icarus, 214,* 377-393. [13] Hiesinger H. et al. (2002) *GRL 29*, 1248-1252. [14] Fassett et al., (2011) *GRL 38*, L10202.